eLIFE elifesciences.org

RESEARCH ARTICLE

Figures and figure supplements

A circuit mechanism for the propagation of waves of muscle contraction in *Drosophila*

Akira Fushiki *et al*

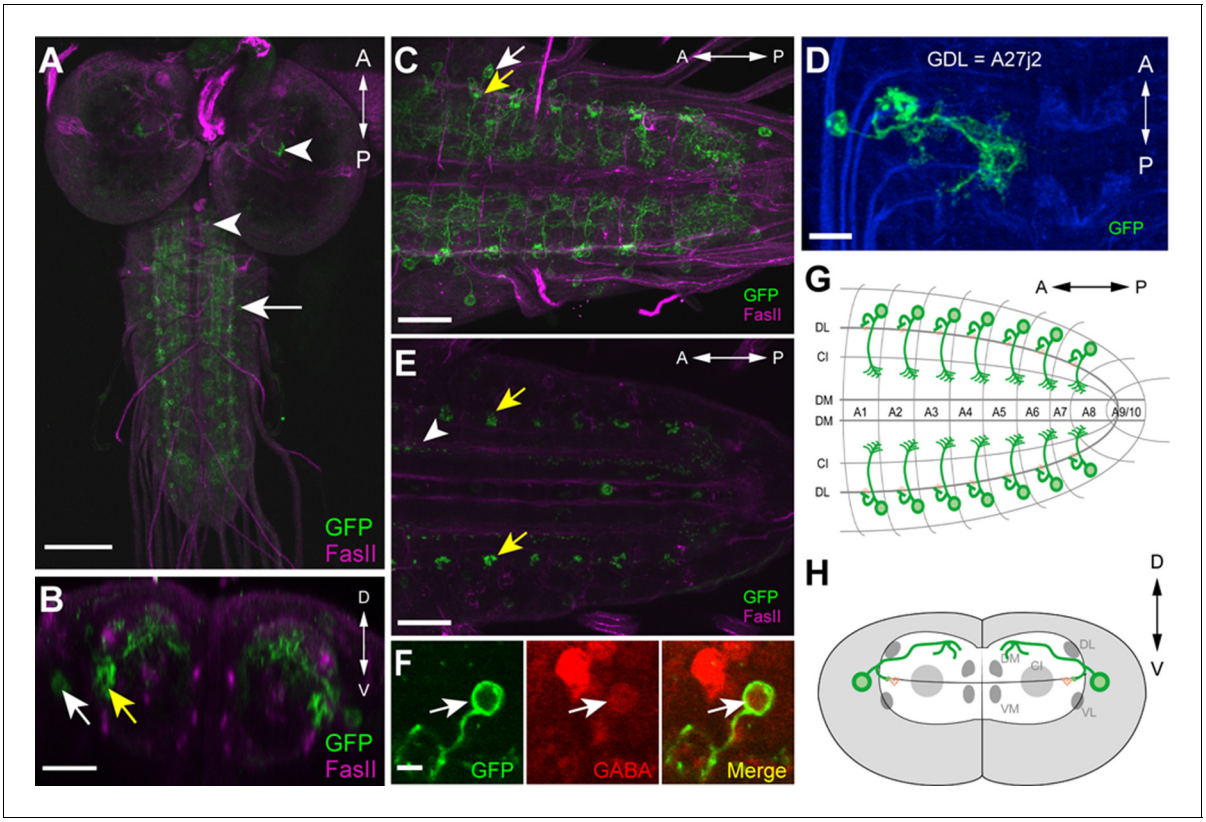

Figure 1. Morphology of GDLs. The *GDL-GAL4* (*9-20-GAL4, iav-GAL80*) drives expression in GDLs and a small number of cells in the brain and SEZ. All panels show dissected third instar larval CNS. (**A–C**) Morphology of GDLs was visualized with *10xUAS-IVS-myr::GFP* reporter expressed by *GDL-GAL4*. Anti-GFP (green) and anti-FasII (magenta) antibodies were used. (**A**) A low magnification view showing *GDL-GAL4* expression in a GDL (arrow) and in a small number of cells in the brain and SEZ (arrowheads). (**B**) A cross sectional view of an abdominal segment. White arrow denotes the cell body of a GDL in a dorsolateral area of the VNC. Yellow arrow denotes the presynaptic terminals of a GDL. (**C**) A dorsal view showing segmentally repeated GDLs in the VNC. Each GDL extends its neurites locally within the segment. Anterior is to the left and posterior is to the right. (**D**) An image of a fluorescently labelled single-cell clone of GDL (courtesy of James W. Truman, HHMI Janelia Research Campus). GDL is also annotated as A27j2. (**E**) *UAS-syt::GFP* was used as a reporter to visualize presynaptic terminals of GDLs (yellow arrows). Signals seen in a medial region (arrowhead) are likely presynaptic terminals of descending neurons from the brain or SEZ (***Figure 7—figure supplement 1B***). (**F**) The cell body of GDLs was positive for GABA. (**G**, **H**) Schematic drawings of GDLs. Scale bar represents 80 μm in (**A**), 30 μm in (**C**, **E**), 20 μm in (**B**), 10 μm in (**D**) and 5 μm in (**F**). (See also ***Figure 1—figure supplement 1***.)

DOI: 10.7554/eLife.13253.003

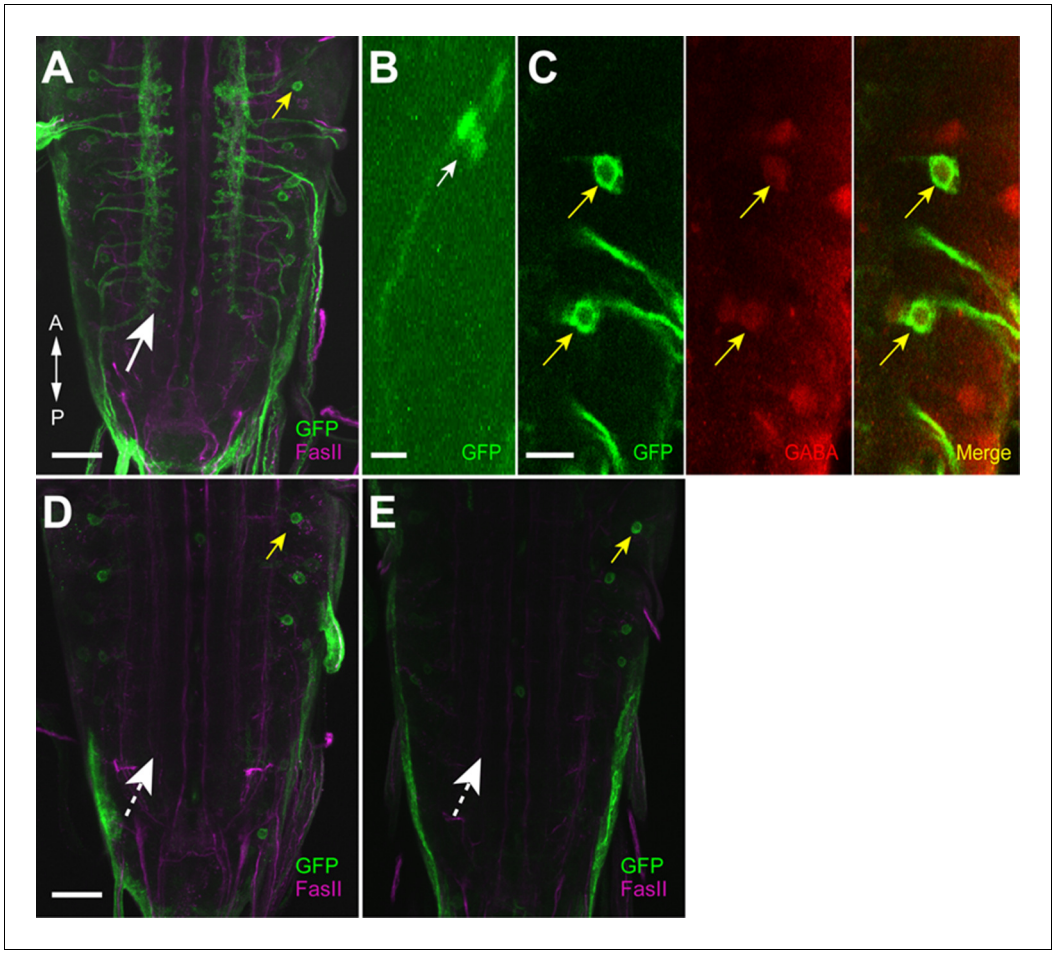

Figure 1—figure supplement 1. Expression driven by *9-20-GAL4* and *inactive (iav)-GAL80*. (**A**, **B**) Expression pattern of the driver line (*9-20-GAL4*) was assessed with *UAS-mCD8::GFP*. (**A**) Expression was seen in the axonal projections of the chordotonal neurons (white arrow) and the soma of a GDL (yellow arrow). (**B**) Expression in the cell body of chordotonal neurons on the body wall. The sensory cilia in chordotonal neurons were observed (white arrow). (**C**) Double-staining for GFP and GABA showing that GDLs were GABAergic (yellow arrows). (**D**, **E**) Expression of *9-20-GAL4* with *iav-GAL80*. Flies were raised at 25°C (**D**) and 29°C (**E**), respectively. No expression was seen in chordotonal neurons (dashed arrows) whereas expression in GDLs was retained (yellow arrows). Scale bar represents 50 μm in (**B**), 30 μm in (**A**, **D**, **E**) and 10 μm in (**C**).

DOI: 10.7554/eLife.13253.004

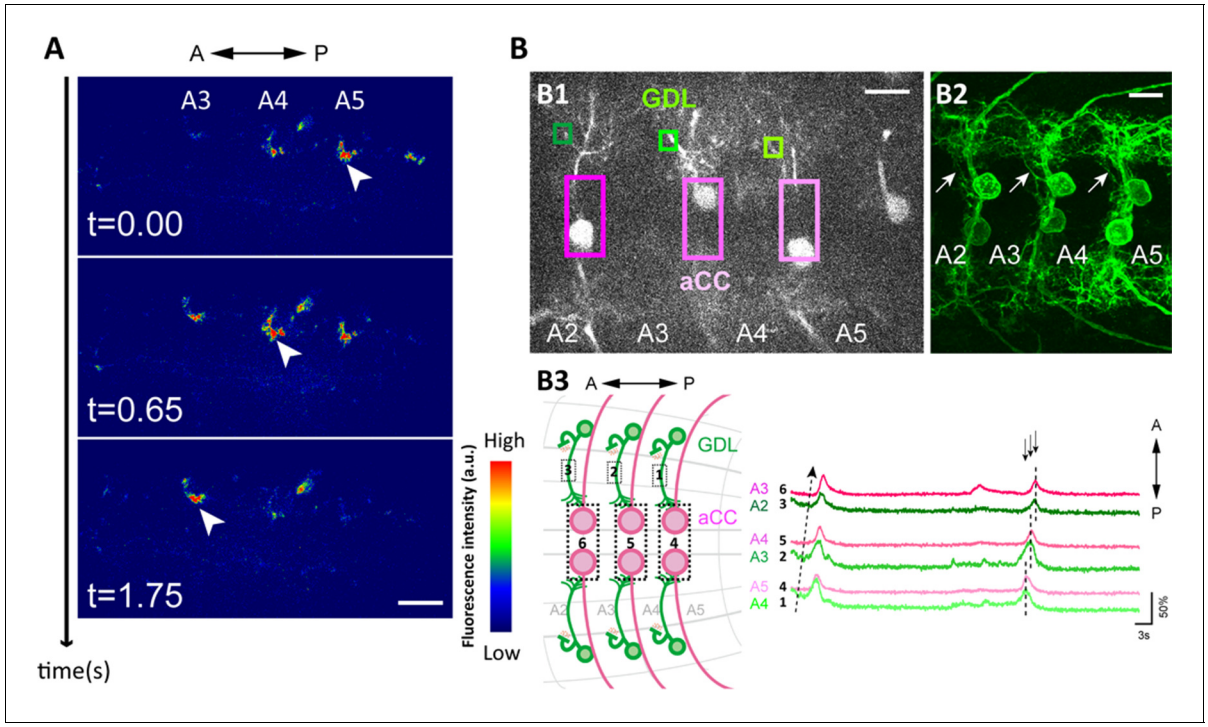

Figure 2. Wave-like activities of GDLs and their phase difference to motor neurons. (**A**) High-resolution calcium imaging of GDL activity in an isolated CNS preparation (*GDL-GAL4>20xUAS-IVS-GCaMP6m*). The increase in the calcium signal in the presynaptic terminals of GDLs propagated from posterior to anterior segments (arrowheads). (**B**) (B1) Regions of interest (ROI) used for the simultaneous calcium imaging of GDLs and aCC motor neurons. We compared the activities between the cell bodies of aCC motor neurons and the dendrites of GDLs (*GDL-GAL4,eve-GAL4>20xUAS-IVS-GCaMP6m*). (B2) Dendrites of GDLs (arrows) can be clearly distinguished from the neurites and cell bodies of aCC motor neurons (*GDL-GAL4,eve-GAL4>10xUAS-IVS-myr::GFP*). (B3) Temporal correlation between the activity of GDLs and aCC motor neurons. Note that activation of GDLs (green) occurs at a similar timing as that of aCC motor neurons in the next posterior segment (arrows, n = 10). Scale bar represents 15 μm in (**A**, **B**). (See also ***Figure 2—figure supplement 1***.)

DOI: 10.7554/eLife.13253.005

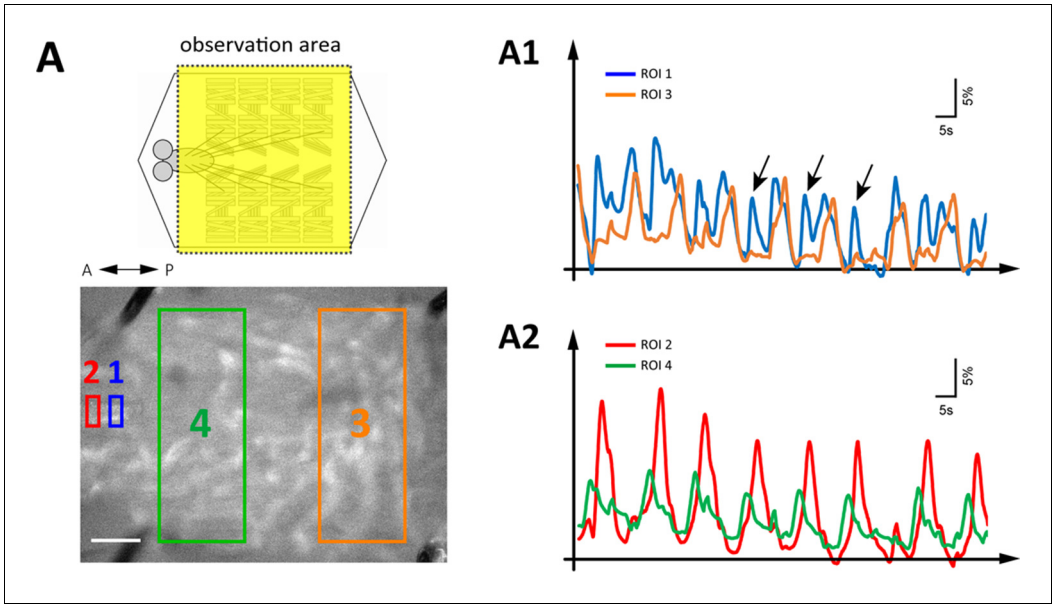

Figure 2—figure supplement 1. Simultaneous imaging of GDLs activity and peristaltic waves. (**A**) GCaMP-based calcium imaging of GDLs during forward movements (*GDL-GAL4>20xUAS-IVS-GCaMP6m*). (A1, A2) Representative fluorescence change of GCaMP6m in GDLs in a posterior (ROI1, blue) and an anterior (ROI2, red) region of the VNC and autofluorescence changes of muscular contractions in a posterior (ROI3, orange) and an anterior (ROI4, green) region of the larva are plotted. The signals of GDLs and segmental muscle contraction propagate at a similar timing. Since the waves of muscle contractions rippled the VNC up and down, the adverse signals can be detected at the posterior VNC (A1, arrows). The amplitude of calcium signals was smoothed (moving average of 30 points). Scale bar represents 250 μm.

DOI: 10.7554/eLife.13253.006

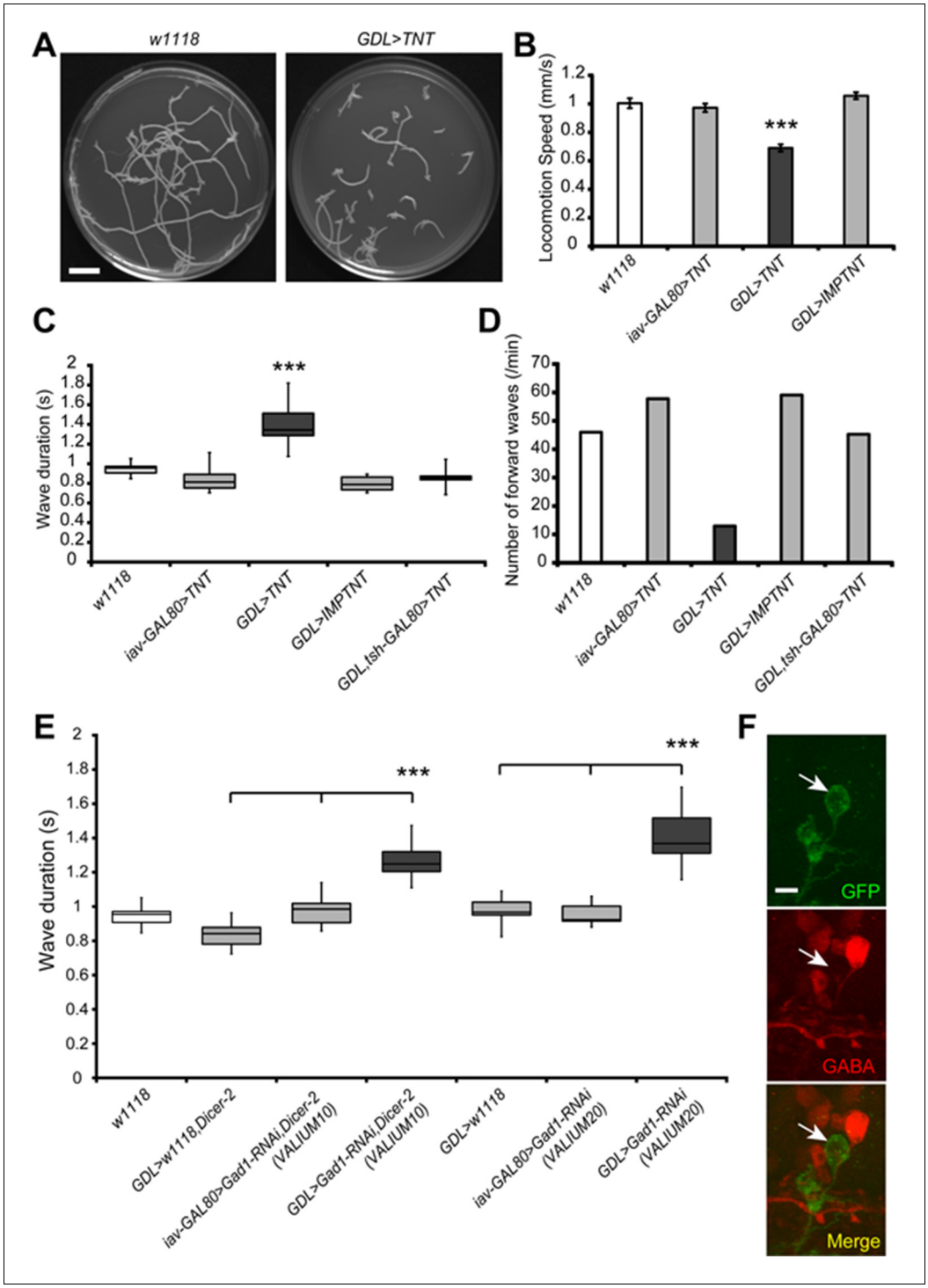

Figure 3. Inhibition of GDLs transmission reduced the speed and frequency of larval peristalsis. (**A**) The path taken by third instar larvae undergoing locomotion for 3 min is shown (left: w^{1118}, right: *GDL-GAL4>UAS-TNT*). (**B**) Inhibition of GDLs with *TNT* decreased the speed of larval locomotion (Locomotion speed, 0.69 ± 0.03 mm/sec [*GDL-GAL4>UAS-TNT*] compared to 1.00 ± 0.04 mm/sec [w^{1118}], 0.97 ± 0.03 mm/sec [*iav-GAL80>UAS-TNT*] and 1.06 ± 0.02 mm/sec [*GDL-GAL4>UAS-IMP(imperfect)TNT*]; p<0.001). (**C**) Expression of *TNT* in *GDL-GAL4* greatly increased the wave duration and the phenotype was rescued by *tsh-GAL80* (Wave duration, 1.40 ± 0.23 sec [*GDL-GAL4>UAS-TNT*] compared to 0.95 ± 0.08 sec [w^{1118}], 0.84 ± 0.12 sec [*iav-GAL80>UAS-TNT*], 0.80 ± 0.07 sec [*GDL-GAL4>UAS-IMP(imperfect)TNT*] and 0.90 ± 0.14 sec [*GDL-GAL4>tsh-GAL80,UAS-TNT*]; p<0.001). (**D**) *TNT*-mediated inhibition also caused a significant decrease in the frequency of larval locomotion (Number of forward

Figure 3 continued on next page

Figure 3 continued

waves, 13.0 waves/min [*GDL-GAL4>UAS-TNT*] compared to 46.0 waves/min [w^{1118}], 57.8 waves/min [*iav-GAL80>UAS-TNT*], 59.1 waves/min [*GDL-GAL4>UAS-IMP(imperfect)TNT*] and 45.3 waves/min [*GDL-GAL4,tsh-GAL80>UAS-TNT*]). (**E**) Expression of two independent *Gad1-RNAi* transgenes in GDLs also increased the wave duration (Wave duration, 1.27 ± 0.1 sec [*GDL-GAL4>Gad1-RNAi(VALIUM10),Dicer-2*] compared to 0.84 ± 0.08 sec [*GDL-GAL4>*w^{1118}*,Dicer-2*] and 0.98 ± 0.09 sec [*iav-GAL80>Gad1-RNAi(VALIUM10),Dicer-2*], 1.41 ± 0.05 sec [*GDL-GAL4>Gad1-RNAi(VALIUM20)*] compared to 0.98 ± 0.03 sec [*GDL-GAL4>*w^{1118}] and 0.96 ± 0.02 sec [*iav-GAL80>Gad1-RNAi(VALIUM20)*]; p<0.001). (**F**) *GDL-GAL4;10xUAS-IVS-myr::GFP* driving *Gad1-RNAi(VALIUM20)* showed a significant reduction of GABA immunoreactivity of GDLs. Box plots in (**C** and **E**) indicate the median value (horizontal line inside the box), 25–75% quartiles (box), and the data range (whiskers). Statistical significance was determined by Student *t*-test or one-way ANOVA followed by Tukey's test for multiple comparisons (***p<0.001). For all conditions in each figure, n = 20 in (**B**) and n = 10 in (**C**, **D**, **E**). Scale bar represents 15 mm in (**A**) and 5 μm in (**F**).

DOI: 10.7554/eLife.13253.009

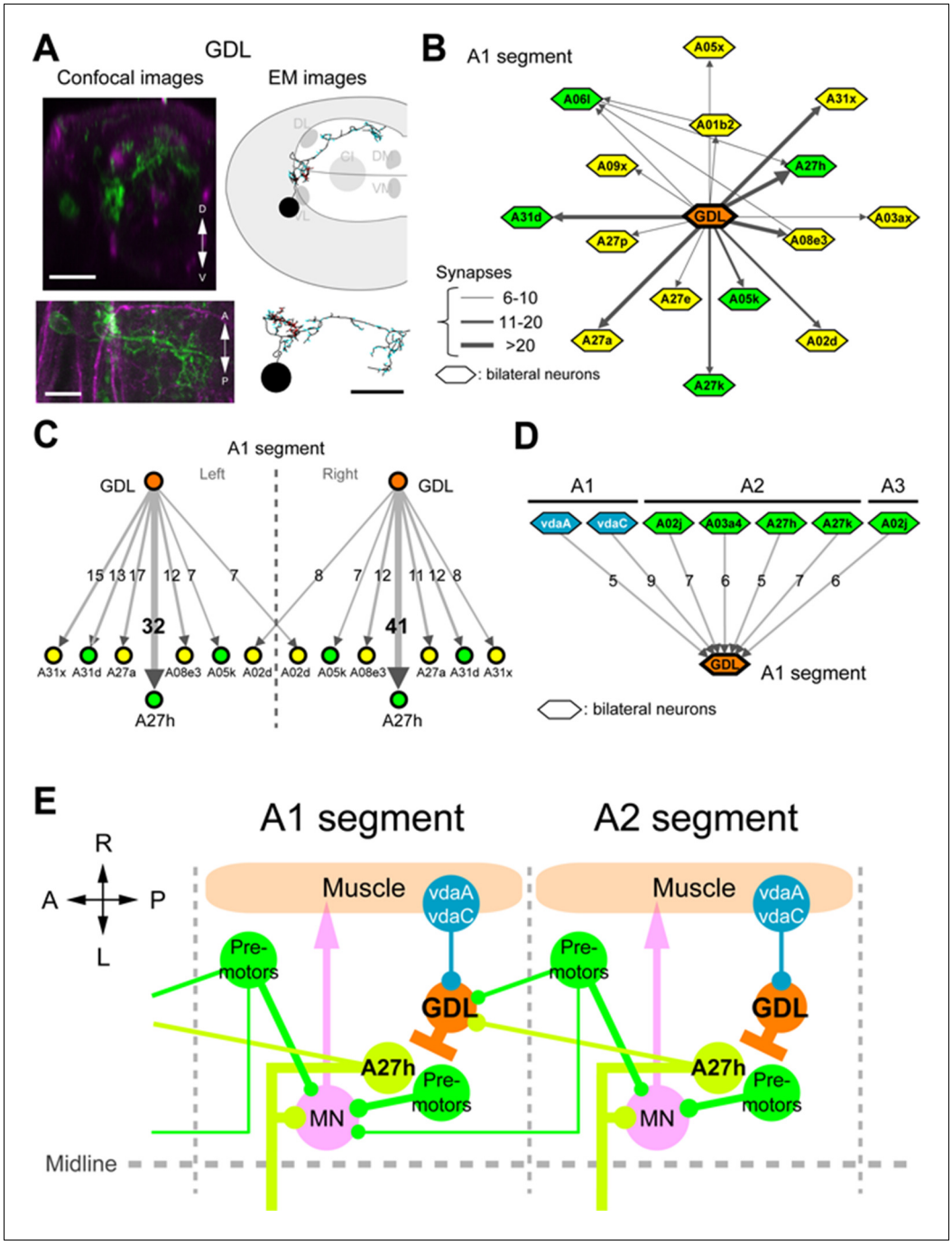

Figure 4. Circuit diagram around GDLs. (**A**) Comparing the confocal images (left) and EM reconstruction (right) of a GDL (top: cross-sectional view, bottom: dorsal view). Postsynaptic sites (cyan) and presynaptic sites (red) are shown in the EM images (right). Scale bar represents 20 μm (upper left), 10 μm (bottom). (**B**) The EM circuit graph of GDLs and their postsynaptic neurons. Hexagonal shape denotes a group of left-right homolog neurons. Connections with less than 6 synapses are not included (green: premotor neurons, yellow: others). (**C**) Major postsynaptic ("downstream") targets of a GDL in the abdominal segment A1. A27h is the strongest synaptic partner of a GDL. Numbers on the directed arrows indicate the number of synapse. (**D**) Major presynaptic ("upstream") targets of a GDL include two dendritic arborization (da) sensory neurons (blue). All other presynaptic targets identified are premotor neurons in the posterior segments (green). (**E**) A circuit model around GDLs. From the wiring diagram, a GDL has connections with several premotor neurons at both upstream and downstream. The symbols: NMJ (arrowheads), putative excitatory synapse (circles), and inhibitory synapse (bars). Thickness corresponds synaptic strength. (See also ***Figure 4—figure supplement 1–3***.)

Figure 4 continued on next page

Figure 4 continued

DOI: 10.7554/eLife.13253.011

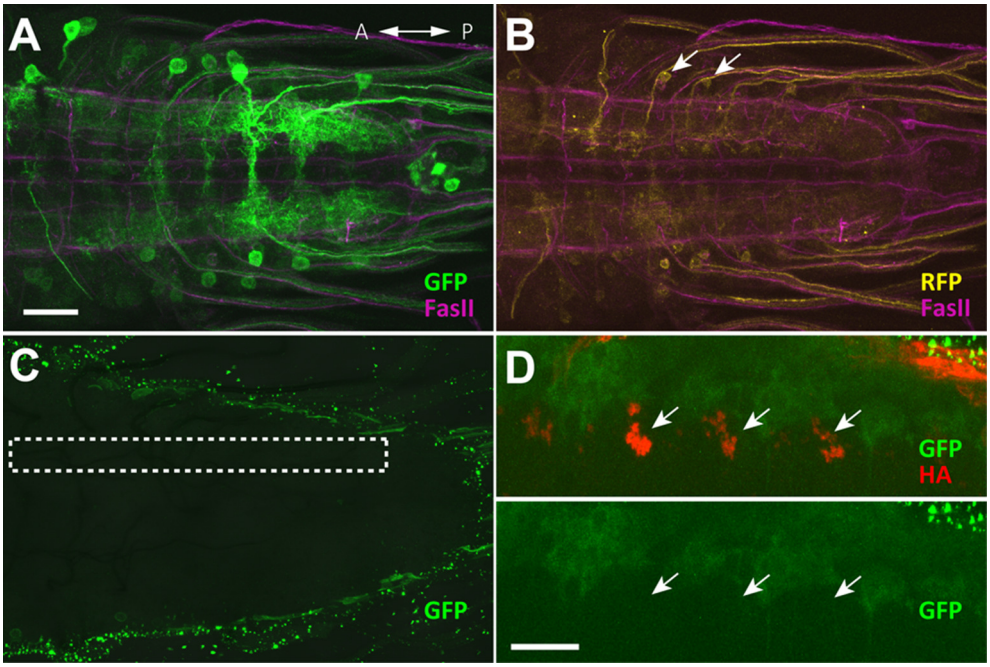

Figure 4—figure supplement 1. No GRASP signal was detected with motor neurons (Related to ***Figure 4***). (**A**–**D**) GRASP experiments. (**A**, **B**) Expression pattern of the driver lines *9-20-GAL4* and *OK6-LexA* were assessed with *10xUAS-IVS-mCD8::RFP,13xLexAop2-mCD8::GFP* and immunostaining with anti-GFP (green), anti-DsRed (yellow), anti-FasII (magenta) antibodies. Arrows denote GDLs in (**B**). (**C**) Results of GRASP (*9-20-GAL4,OK6-LexA>OK6-LexA, LexAop-CD4::spGFP11;UAS-CD4::spGFP1-10*) visualized by immunolabeling with a monoclonal antibody against GFP (Sigma). No GRASP signal was detected. Dashed box indicates the positions of the presynaptic sites of GDLs. (**D**) Syt::HA was coexpressed with GRASP reporters to assess the precise location of GDL presynaptic terminals (*UAS-syt::HA;9-20-GAL4,OK6-LexA>OK6-LexA,LexAop-CD4::spGFP11;UAS-CD4::spGFP1-10*). However, no GRASP signals were observed at the terminals (arrows). Scale bar represents 30 μm in (**A**–**C**) and 20 μm in (**D**).
DOI: 10.7554/eLife.13253.012

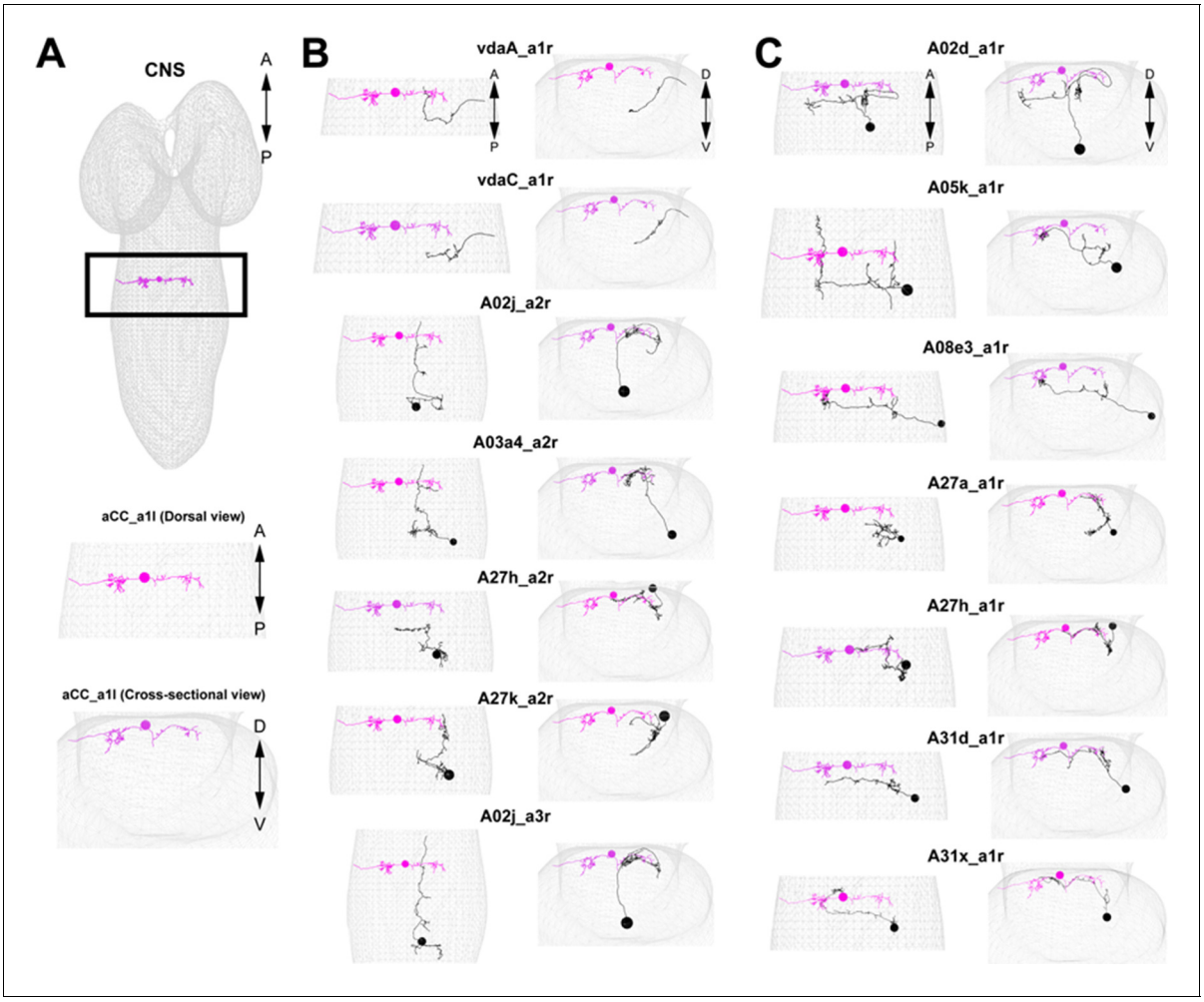

Figure 4—figure supplement 2. Morphology of the major presynaptic and postsynaptic neurons of GDL. (**A**) An aCC motor neuron in A1 segment is shown in the comprehensive EM dataset. We use the position of the aCC for reference in (B) and (C). (**B**) Seven major presynaptic targets of a GDL (A1: vdaA, vdaC, A2: A02j, A03a4, A27h, A27k, A3: A02j). (**C**) Seven major postsynaptic targets of a GDL (A02d, A05k, A08e3, A27a, A27h, A31d, A31x: all of the neurons exist at A1 segment).

DOI: 10.7554/eLife.13253.013

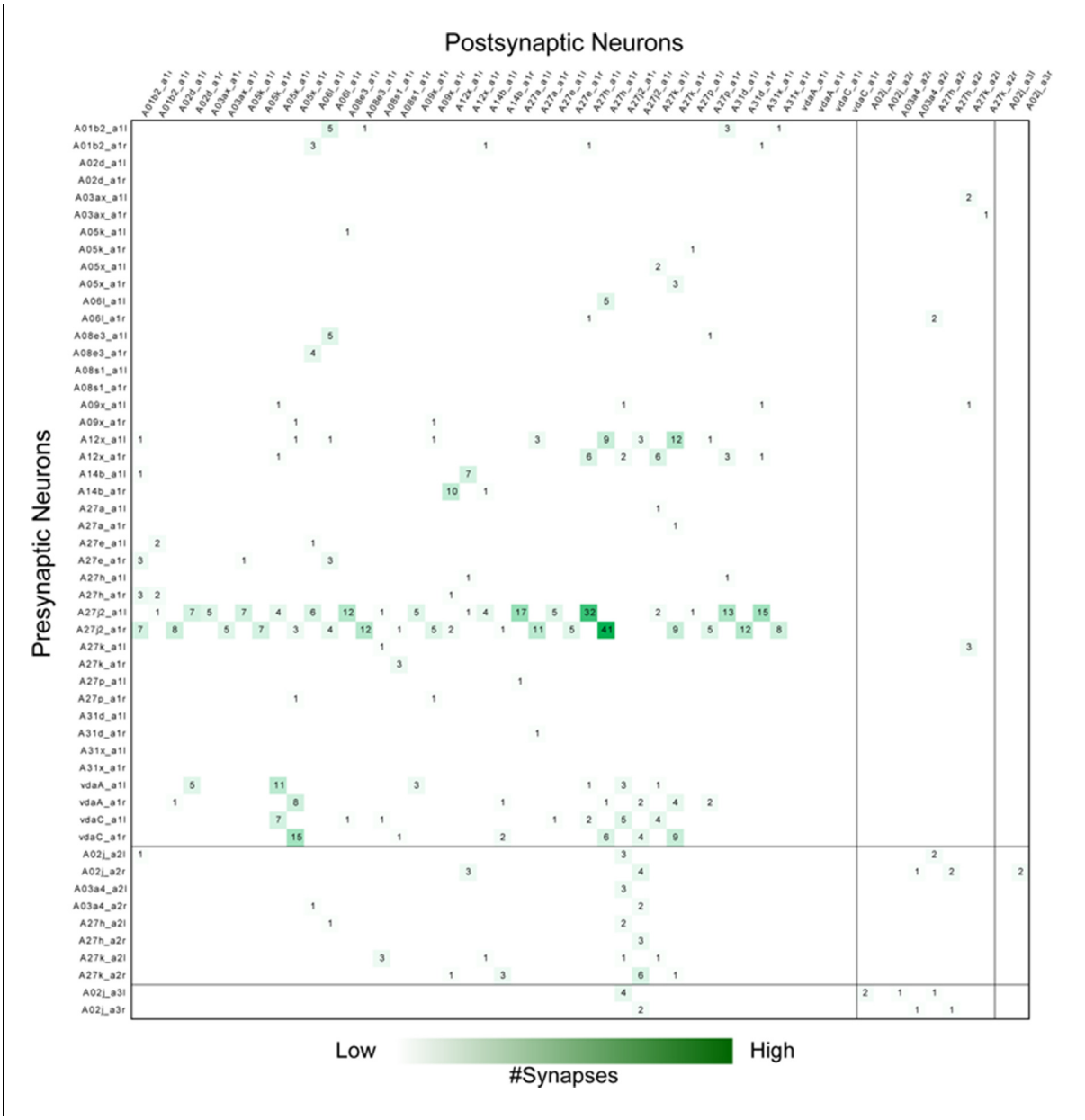

Figure 4—figure supplement 3. Adjacency matrix for GDL circuits. Each row and column represents a neuron's' pre- and post- synaptic contacts, respectively. The number in the matrix is the synapse number between the target neurons and their partners. Neurons are grouped by segments. GDLs are annotated as "A27j2_a1" in this figure.

DOI: 10.7554/eLife.13253.014

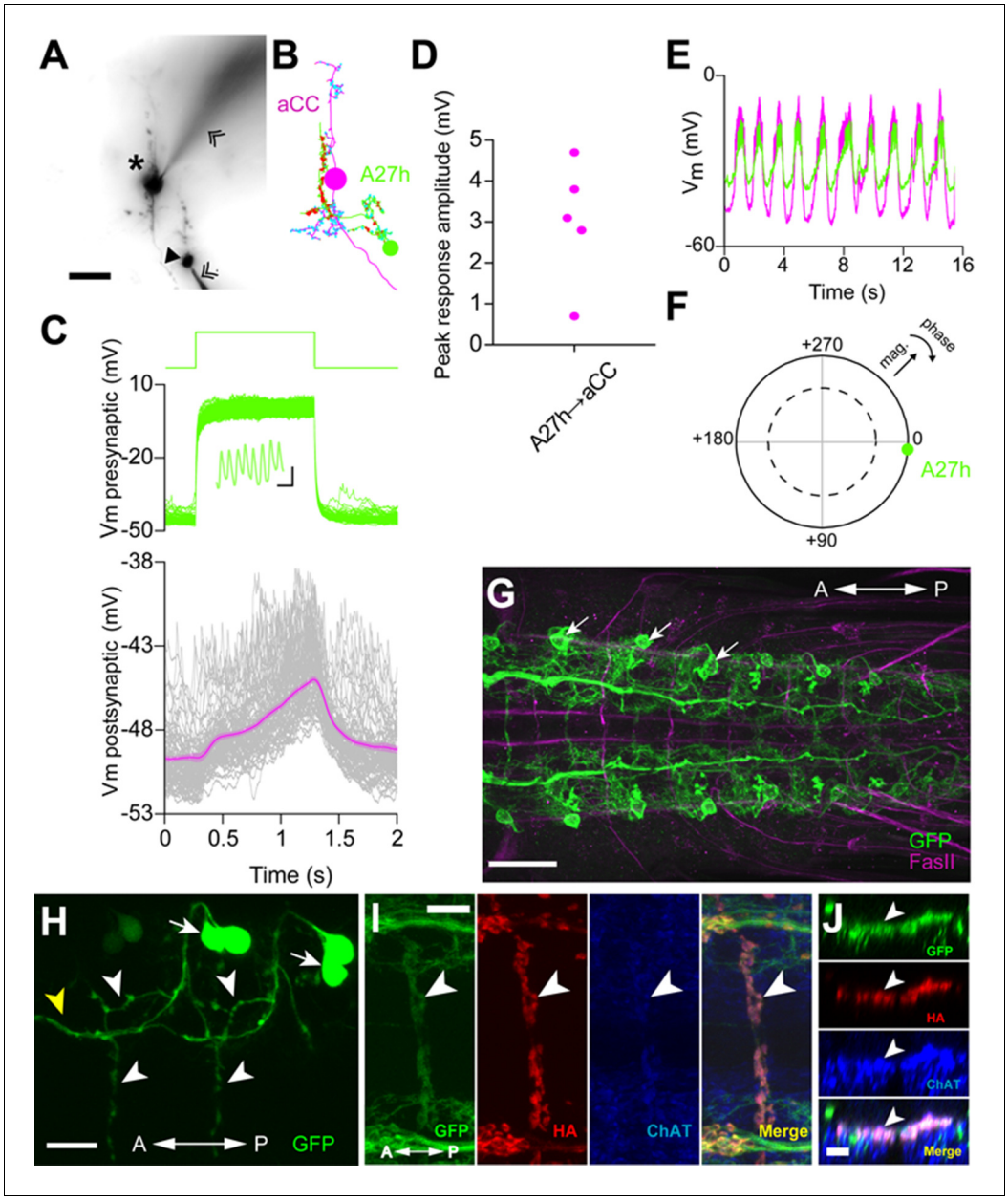

Figure 5. A27h is an excitatory premotor interneuron. (**A**) An example of a paired recording of an aCC motor neuron (asterisk) and a presynaptic A27h (arrowhead) dye-filled with Alexa 568 in the intracellular recording solution. Recording electrodes are indicated with chevrons. (**B**) EM reconstructions of aCC (magenta) and A27h (green). Input synapses are labeled in cyan, output synapses in red. (**C**) A current command (50 pA) results in A27h firing action potentials (see zoomed-in view in inset, scale bar indicates 10 ms, 0.5 mV), which efficiently drives the postsynaptic aCC motor neuron (magenta trace depicts mean of 100 trials ± SEM). (**D**) The maximum voltage response in aCC to presynaptic stimulation. Each point indicates the mean response of 100 trials of current injection in a different cell. (**E**) Endogenous activity patterns of these two cells, with each burst corresponding to a peristaltic wave. (**F**) Phase plot describing the coherency between the two cells, with magnitude of coherence depicted as the distance from the center, and the phase shift as deviation from 0° (with aCC at 0°). Dashed line indicates $\alpha = 0.05$ for coherence magnitude statistically deviating from 0. (**G**) Expression driven by *R36G02-GAL4*. Assessed with the *10xUAS-IVS-myr::GFP* reporter and immunostaining with anti-GFP (green) and anti-FasII (magenta) antibodies. Strong expression was seen in A27h (arrows) and a small number of other cells in the VNC. (**H**) Photolabeling of A27h neurons. A flash of near-UV light (~405 nm) was applied to a dorso-lateral region of the VNC dissected from a *R36G02-GAL4>UAS-C3PA* larva, to label A27h and neighboring cells and their axonal arborization. The cell body of A27h can be uniquely identified for its stereotypic relative position to other cells

Figure 5 continued on next page

Figure 5 continued

(arrows); white arrowheads, axons of A27h; yellow arrowhead, an axon of a different cell. (**I**, **J**) A27h presynaptic terminals (arrowheads) express ChAT. Triple labeling for membrane-GFP (green), presynaptic marker (red) and ChAT (blue) (in *R36G02-GAL4>UAS-syt::HA;10xUAS-IVS-myr::GFP*). Dorsal (**I**) and cross-sectional (**J**) view are shown. Scale bar represents 30 μm in (**G**), 20 μm in (**A**, **H**), 10 μm in (**I**) and 5 μm in (**J**). (See also ***Figure 5—figure supplement 1***, ***2***).

DOI: 10.7554/eLife.13253.015

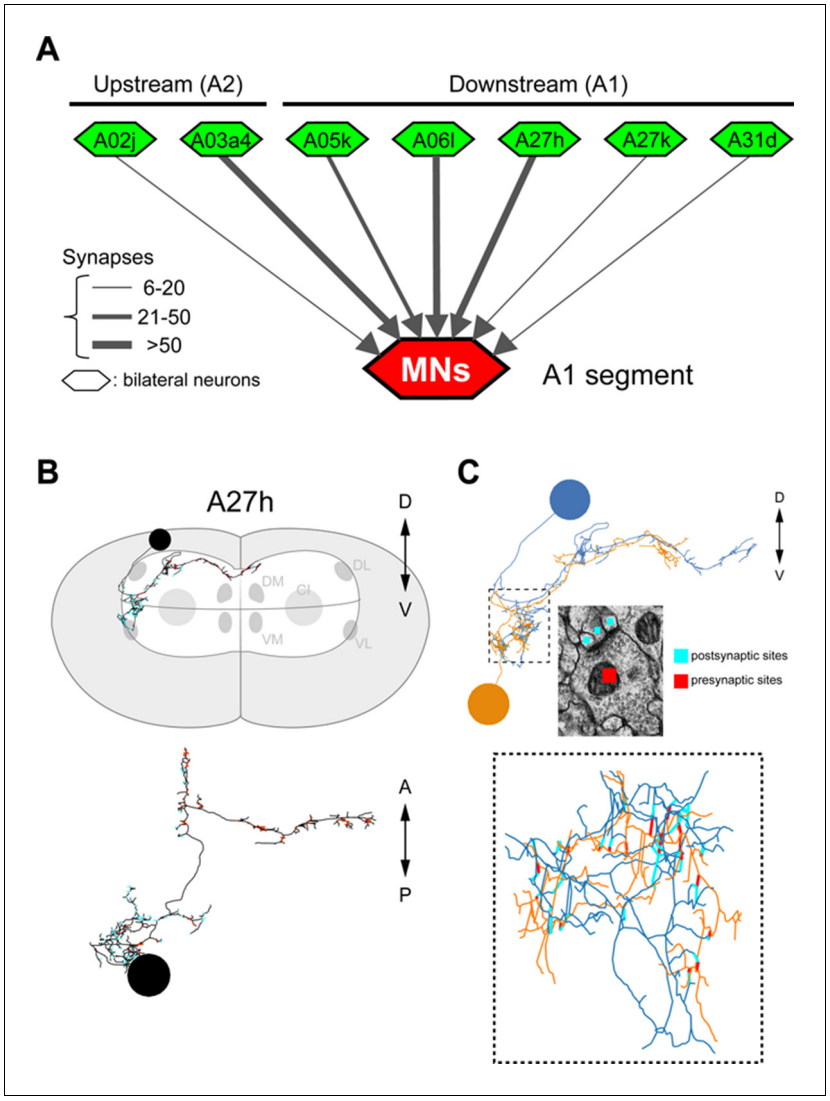

Figure 5—figure supplement 1. The connectivity of premotor neurons (Related to ***Figure 5***). (**A**) Some presynaptic ("upstream") and postsynaptic ("downstream") neurons are premotor neurons. (**B**) Morphological features of A27h. The cell body of A27h is in the most dorsal part of the VNC and the axon extends to the anterior midline. (**C**) GDL (orange) and A27h (blue) are connected to each other in a lateral-medial part of the VNC.
DOI: 10.7554/eLife.13253.016

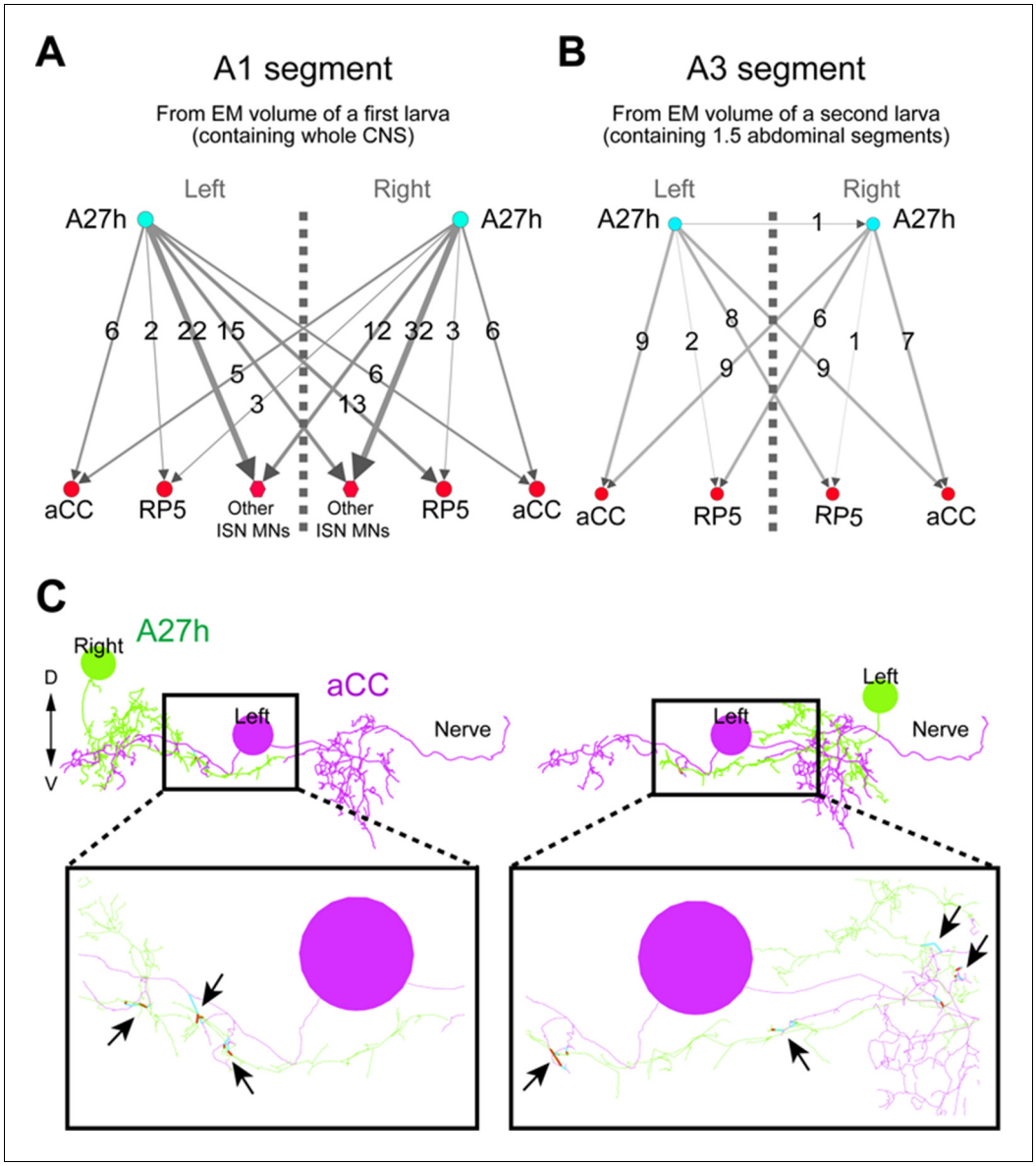

Figure 5—figure supplement 2. Bilateral A27h connection to motor neurons was confirmed in two independent EM volumes. (**A**, **B**) The bilateral connectivity between A27h, aCC and RP5 was confirmed in two different EM volumes (left: a first larva containing whole CNS, right: a second larva containing 1.5 abdominal segments). (**C**) Both left and right A27h neurons were connected to near-soma positions of the left (or right) aCC motor neuron. Arrows denote the synaptic connections between A27h neurons (green) and an aCC motor neuron (magenta).
DOI: 10.7554/eLife.13253.017

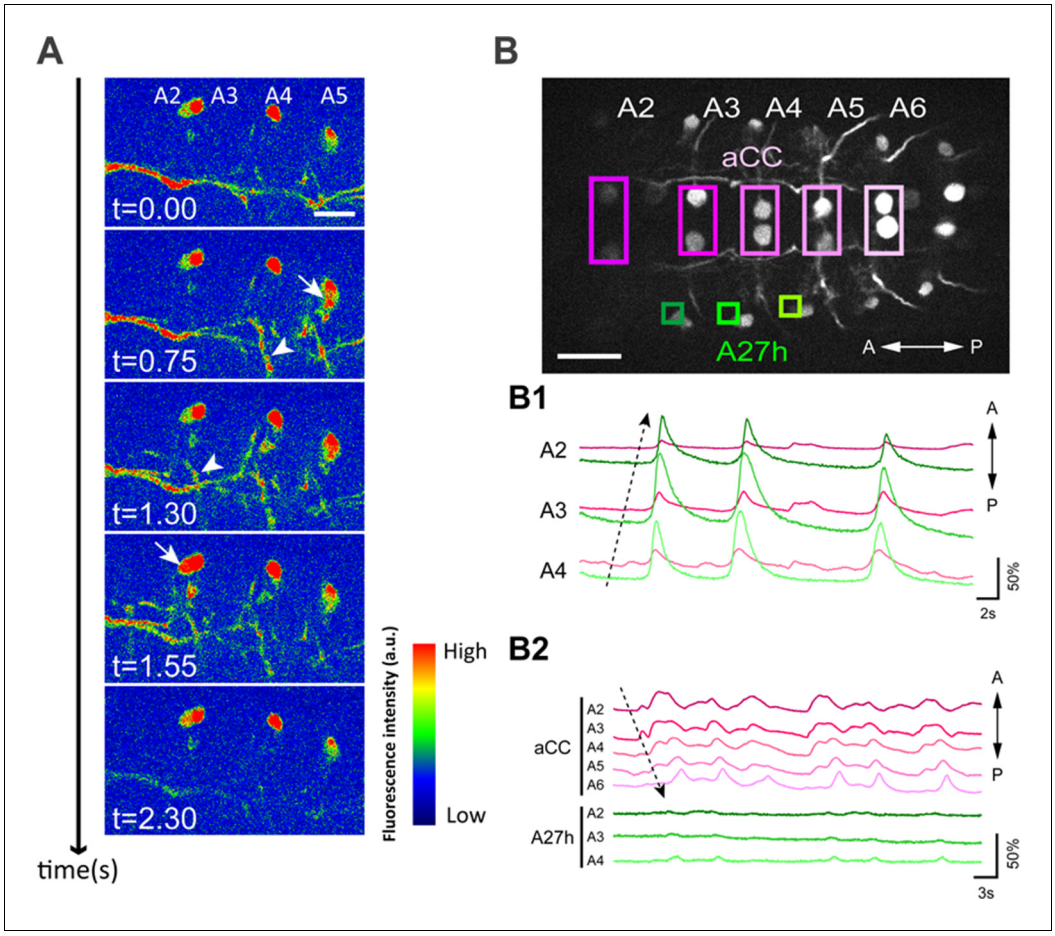

Figure 6. A27h participates in forward motor activity. (**A**) Calcium imaging of A27h (in *R36G02-GAL4>20xUAS-IVS-GCaMP6m*). Arrows denote the cell bodies of A27h neurons and arrowheads axons of A27h neurons. (**B**) Simultaneous imaging of the activity of A27h neurons (green) and aCC motor neurons (magenta) (in *R36G02-GAL4,eve-GAL4>20xUAS-IVS-GCaMP6m*). The top panel shows the region of interests (ROI) used for the analyses. (B1, 2) Dashed arrows denote the directions of motor activity. A27h was activated only during forward movement (B1) but not backward movement (B2). Scale bar represents 30 μm in (**B**) and 15 μm in (**A**).
DOI: 10.7554/eLife.13253.019

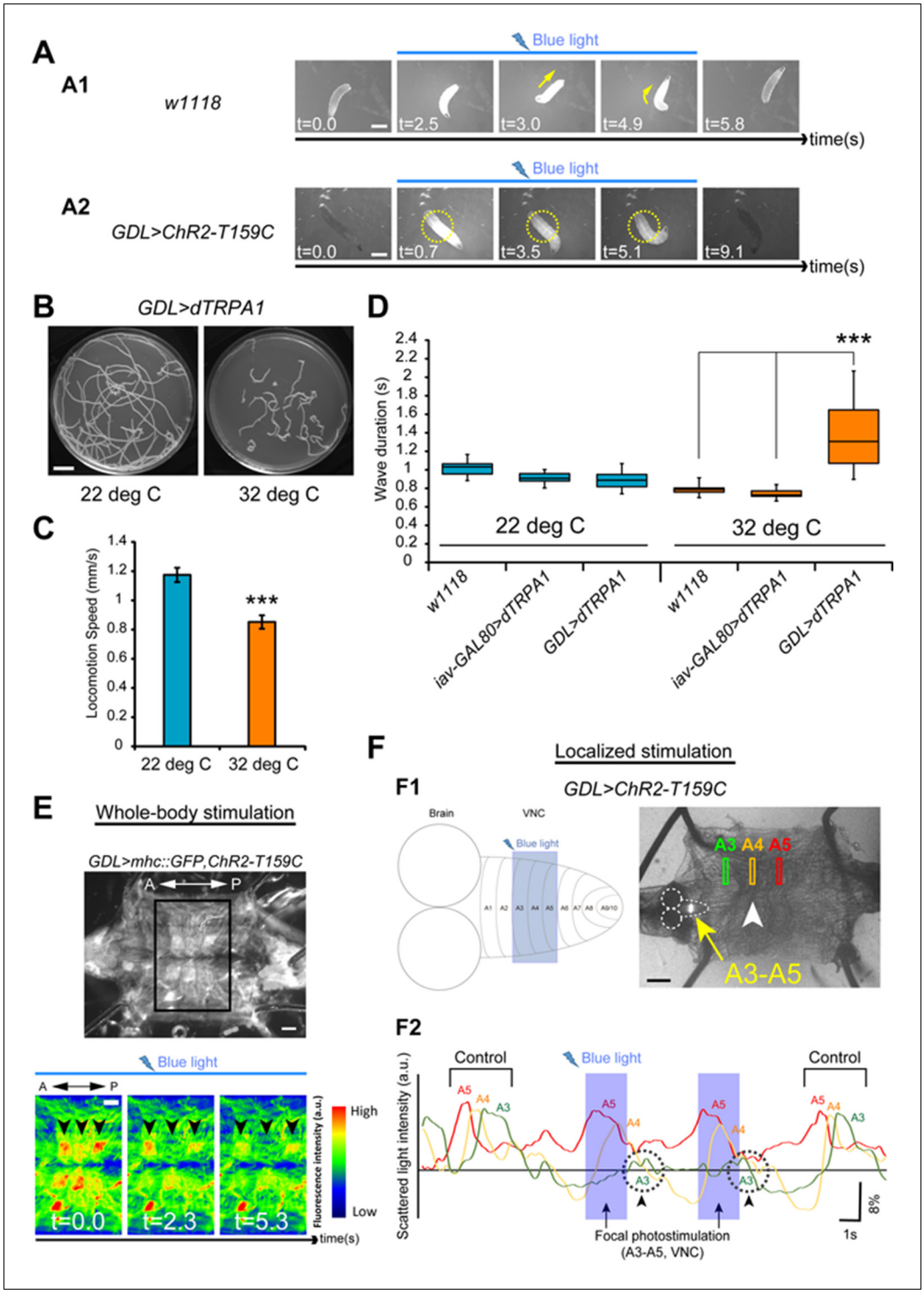

Figure 7. Optical perturbation of the activity of GDLs disrupts the peristalsis. (**A**) Behavioral responses induced by optogenetic activation of *GDL-GAL4*-expressing neurons (A1) A wild-type larva. Illumination with blue light (~480 nm) induced light-avoidance behaviors such as backward movement and head turning. (A2) Channelrhodopsin-2 (ChR2)-mediated activation of GDLs completely immobilized the abdominal segments of the larva (yellow dashed circles; 10 of 10 larvae [*GDL-GAL4>UAS-ChR2-T159C*] compared to 0 of 8 cases in the control larvae [w^{1118}*>UAS-ChR2-T159C*]). (**B–D**) Larvae expressing dTRPA1 in *GDL-GAL4* showed locomotion defects at a restrictive temperature. Traces (**B**), locomotion speed (**C**) and wave duration (**D**) at permissive and restrictive temperatures are shown (C; Locomotion speed, 0.85 ± 0.05 mm/sec compared to 1.17 ± 0.05 mm/sec in the

Figure 7 continued on next page

Figure 7 continued

control larvae, the larvae with the same genotype at a permissive temperature (22°C), D; Wave duration, 1.42 ± 0.43 sec [*GDL-GAL4>UAS-dTRPA1*] compared to 0.79 ± 0.06 sec [w^{1118}] and 0.74 ± 0.05 sec [*iav-GAL80>UAS-dTRPA1*]; p<0.001. Note that larvae normally crawl faster at 32°C than at 22°C). For all conditions in each figure, n = 20 in (**C**) and n = 10 in (**D**). (**E**) A dissected larva expressing ChR2-T159C in *GDL-GAL4* and mhc::GFP in muscles (*GDL-GAL4>mhc::GFP, UAS-ChR2-T159C*). When blue light was applied during peristalsis, contracted muscles became relaxed (n = 12). (**F**) (F1) Localized photostimulation was applied to an anterior portion of the VNC (around A3-A5, yellow arrow) during peristalsis. Arrowhead denotes the contracting segments at this moment. (F2) Muscular movement was examined by using the scattered light changes. The light intensity change in muscles in A3-A5 is plotted. In this example, the peristaltic wave halted at A3 (dashed circle with arrowheads). Statistical significance was determined by Student's *t*-test or one-way ANOVA followed by Tukey's test for multiple comparisons (***p<0.001). Scale bar represents 15 mm in (**C**), 9 mm in (**A**), 250 μm in (**F**) and 200 μm in (**B**). (See also ***Figure 7—figure supplement 1***.)

DOI: 10.7554/eLife.13253.021

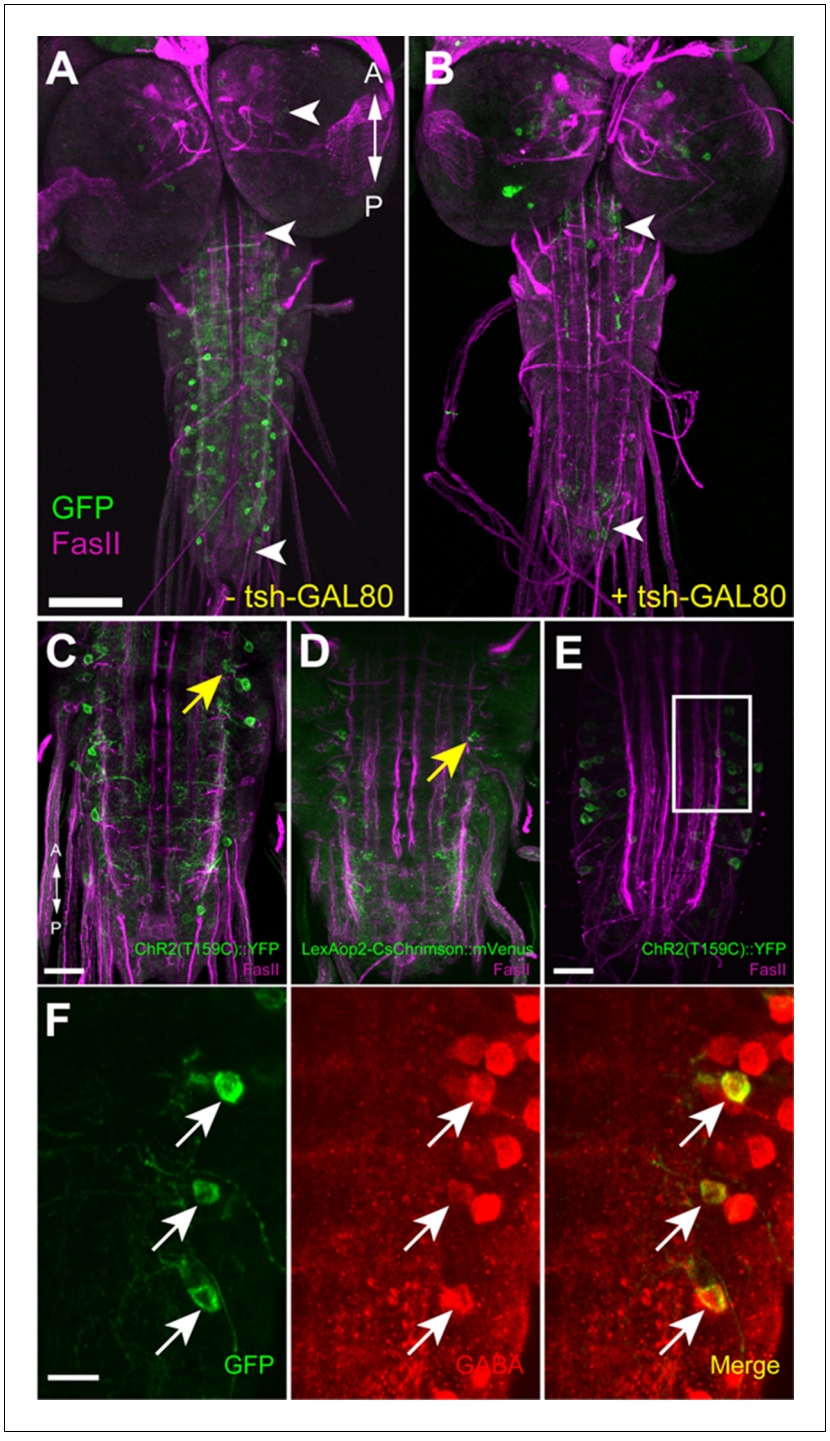

Figure 7—figure supplement 1. Confirmation of the expression of ChR2 in GDLs. Expression of ChR2 reporters, ChR2(T159C)::YFP (**A**, **B**, **C**, **E**, **F**) driven by *GDL-GAL4,* and CsChrimson::mVenus driven by *R15C11-LexA* (**D**), in GDLs were confirmed. (**A**, **B**) *tsh-GAL80* specifically eliminates *GDL-GAL4*-mediated expression in the VNC, without affecting the expression in cells in the brain, SEZ and the terminal (arrowheads). (**C**–**F**) Yellow and white arrows denote presynaptic terminals and cell bodies of GDLs, respectively. (**A**–**D**) Third instar, (**E**, **F**) First instar. (**F**) is a high magnification image of (**E**). Scale bar represents 80 μm in (**A**, **B**), 30 μm in (**C**, **D**), 20 μm in (**E**) and 10 μm in (**F**).

DOI: 10.7554/eLife.13253.022

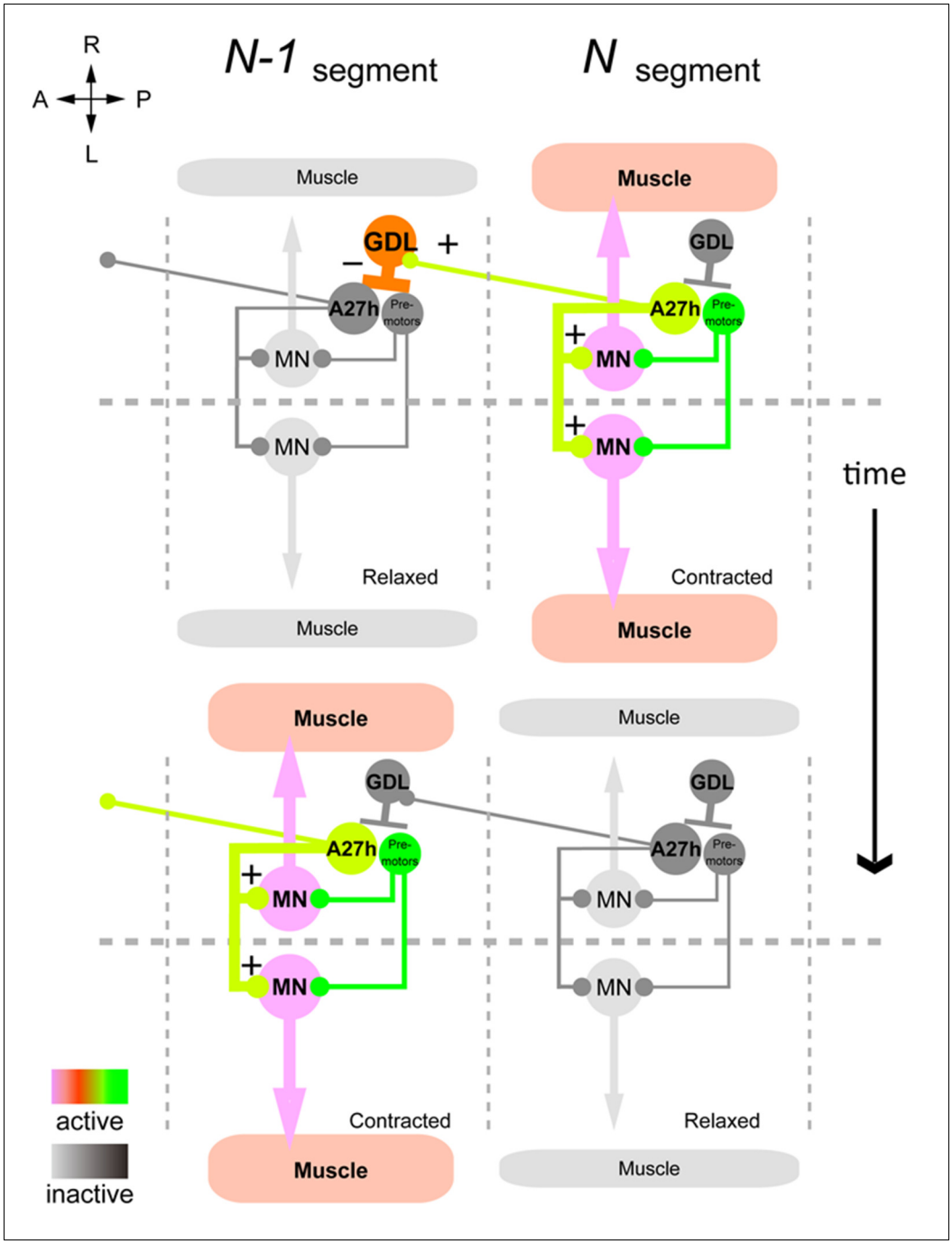

Figure 8. Summary of the GDL circuit. The information flow in the GDL-A27h premotor circuit. At a time point during forward peristalsis when A27h in segment *N* is active and driving motor activity in the segment, GDL in the next anterior segment *N-1* is active and inhibits the activity of A27h and the downstream motor activity in the segment. As the motor wave propagates anteriorly and motor activity in segment *N* declines, so does the GDL in segment *N-1*, thus releasing the target A27h from its inhibition (gray: inactive, other colors: active). (See also ***Figure 8—figure supplement 1***.)

DOI: 10.7554/eLife.13253.025

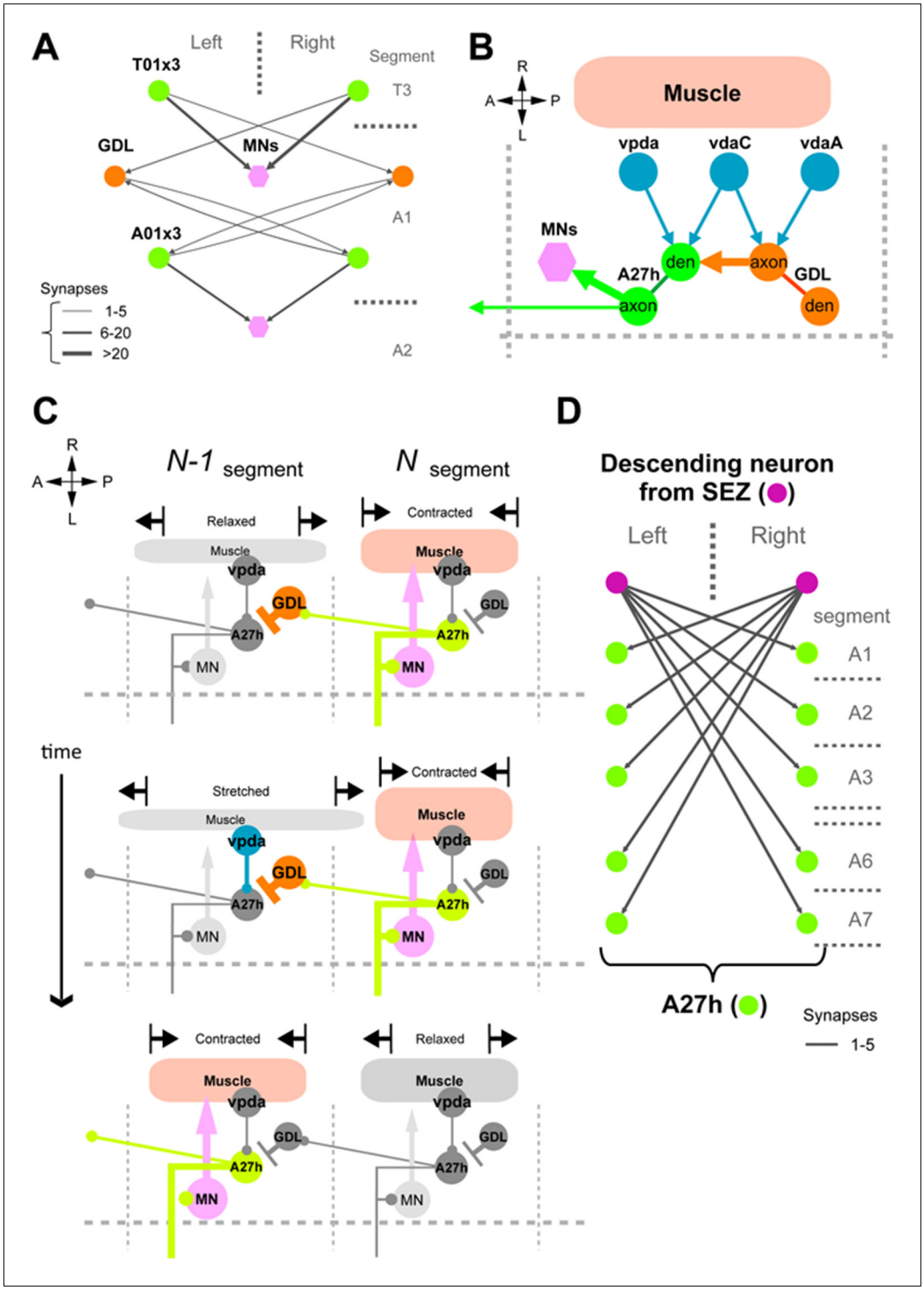

Figure 8—figure supplement 1. A proposed circuit mechanism for moderating peristaltic locomotion. (**A**, **B**, **D**) EM reconstructions. (**A**) A candidate neuron for backward peristalsis. T01x3 is a homolog of A01x3 in thoracic segment. (**B**) A proprioceptive (vpda) and two other sensory neurons (vdaA and vdaC) synapse axo-dendritically onto A27h and axo-axonically onto a GDL of their own segment. (**C**) A proposed model of sensory feedback (per hemisegment). Note that the feedback have two simultaneous effects: promote the contraction of its own segment ahead of the wave, and then relaxation (or stretch) of the next anterior segment. (**D**) A descending neuron from the SEZ has connections with A27h neurons at each segment.

DOI: 10.7554/eLife.13253.026

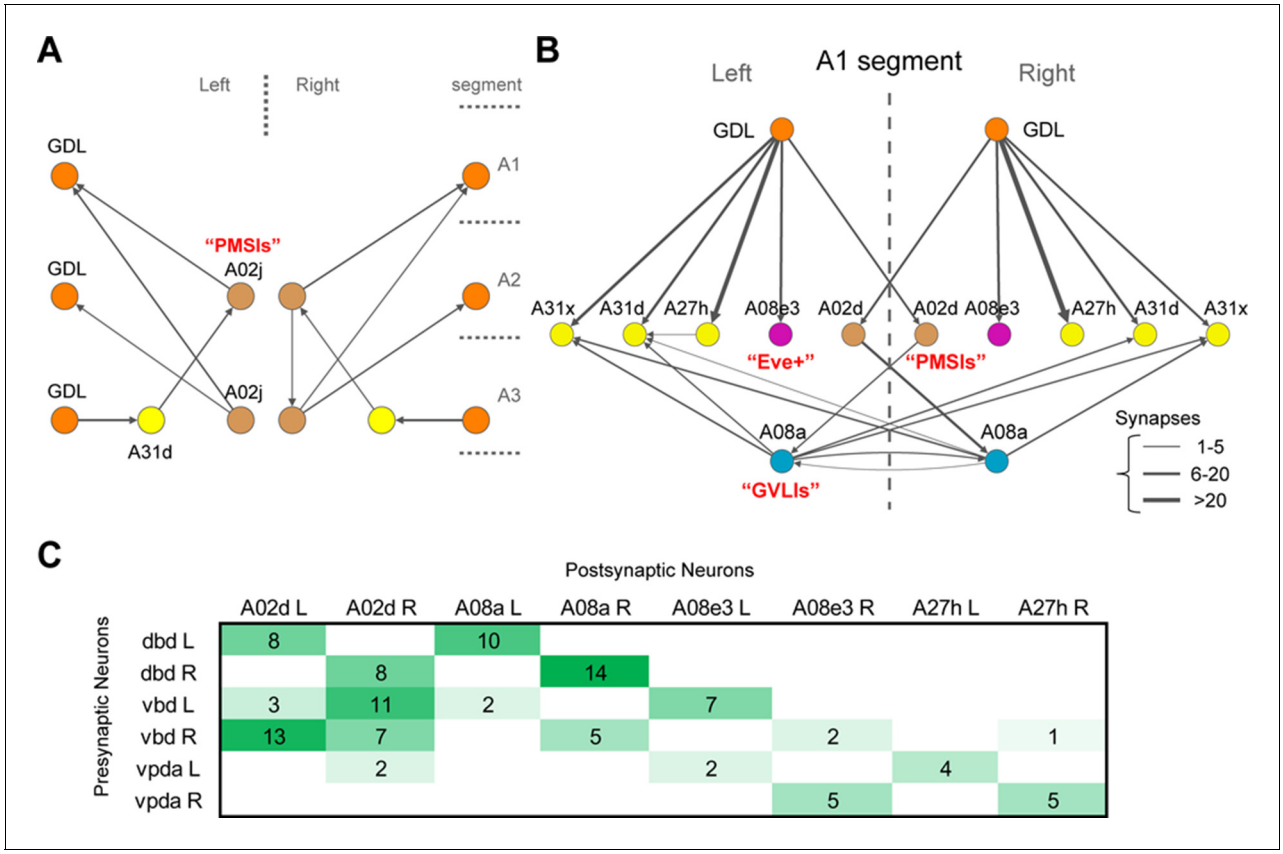

Figure 8—figure supplement 2. Synaptic relations of GDL and A27h with known larval interneurons. (**A**) One of the PMSI neurons (glutamatergic neurons involved in the speed regulation; [***Kohsaka et al., 2014***]), named A02j, relates GDLs to each other across abdominal segments. In particular, A02j synapses onto the GDLs of the two segments anterior to its own segment, potentially starting the excitatory drive over GDLs to promote the relaxation of segments anterior to the muscle contraction wave. Additionally, A02j synapses directly onto some motor neurons of the segments anterior to its own segment (not shown), with potentially an inhibitory effect as shown in (***Kohsaka et al., 2014***). Interestingly, A02j in one segment might promote the disinhibition of its anterior homologs, given than GDL, a GABAergic neuron, synapses onto a segment-local putatively GABAergic neuron (A31d; similar morphology and belonging to the same lineage as the GABAergic neurons A31b and A31k [***Schneider-Mizell et al., in press***]). (**B**) The GDL-A27h circuit interacts with neurons known to affect the speed of locomotion (PMSIs and GVLIs). A02d is a PMSI neuron (***Kohsaka et al., 2014***) that receives inputs from GDL and in turn synapses onto the A08a neuron (a GVLI; [***Itakura et al., 2015***]). A08a, in turn, synapses onto two putatively GABAergic neurons (A31d and A31x). This circuit suggests that GDL prevents A02d from driving A08a, which could potentially underlie the observed activation pattern of A08a, which is active two segments posterior to the forward-moving peristaltic wave (***Itakura et al., 2015***). We did not observe synapses between A08a and motor neurons. Furthermore, GDL might provide inhibition ipsilaterally to the contralaterally projecting, Eve-Skipped+ neuron A08e3, which is necessary for maintaining bilaterally symmetric muscle contraction amplitude (***Heckscher et al., 2015***). This suggests a role for GDL in the regulation of posture adjustment, and therefore a close relationship between the circuits for wave propagation and the circuits for ensuring symmetrical muscle contractions in forward locomotion. (**C**) The connectivity matrix between proprioceptive sensory neurons and A02d (one of the PMSIs), A08a (GVLIs), and A08e3 (one of the Even-Skipped+ neurons).

DOI: 10.7554/eLife.13253.027